Accurate energies of nS, nP, nD, nF, and nG levels of neutral cesium

K.-H. Weber* and Craig J. Sansonetti

National Measurement Laboratory, National Bureau of Standards, Gaithersburg, Maryland 20899
(Received 22 December 1986)

Extensive measurements have been performed to determine the absolute energies of the $n\,^2S_{1/2}$ ($n=8-31$), $n\,^2P_{1/2}$ ($n=6,9-80$), $n\,^2D_{5/2}$ ($n=5,7-36$), $n\,^2F_{5/2}$ ($n=6-65$), and $n\,^2G_{7/2}$ ($n=6-54$) levels of Cs by using nonresonant and resonantly enhanced Doppler-free two-photon spectroscopy. The excitation mechanisms employed include resonantly enhanced dipole-quadrupole and quadrupole-quadrupole transitions. All energies were measured directly with respect to the $6\,^2S_{1/2}$ ground state. The laser wavelengths were measured by high-precision Fabry-Perot interferometry yielding an uncertainty of 0.0002 cm^{-1} for most Cs levels. Ionization energies derived by fitting the modified Ritz formula to each of the five series observed coincide within 0.00005 cm^{-1}. Taking account of possible systematic errors, the Cs ionization energy is 31406.46766(15) cm^{-1}.

INTRODUCTION

During the last 37 years there have been many determinations of energy levels of neutral cesium using classical methods of grating and interferometric spectroscopy.[1-8] In recent experiments Doppler-free laser spectroscopy has been used to investigate Cs levels of even parity,[9-12] and the $6\,^2P_{3/2}$ level has been determined by measuring the D_2 line of Cs in an atomic beam;[13] but prior to our current work, the energies of other odd-parity states and high-angular-momentum states of Cs have not been determined by optical sub-Doppler spectroscopy. Although reported Rydberg-state and ionization energies of the other heavy alkali metals show reasonable consistency,[14-18] the recent data for Cs disagree far beyond their stated uncertainties.[11,12]

Resonantly enhanced Doppler-free multiphoton excitation was first discussed and demonstrated in Na by Bjorkholm and Liao.[19,20] The method was recently employed by Sansonetti and Lorenzen[21] to measure fine-structure intervals in odd-parity states of Cs.

In this work we have applied resonantly enhanced two-photon spectroscopy to the precise determination of energy levels. Using the $5\,^2D_{3/2}$ level as a resonant intermediate state we have made Doppler-free observations of the $^2P_{1/2,3/2}$, $^2F_{5/2}$, and $^2G_{7/2}$ levels of neutral Cs. Our experimental method permitted us to eliminate the large Doppler shifts which can occur in resonantly enhanced two-photon absorption and to determine the energy of these excited states with direct reference to the ground state. We have also made new measurements of the $^2S_{1/2}$ and $^2D_{5/2}$ series and made a precise determination of the Cs ionization energy.

EXPERIMENT

Excitation

Two excitation schemes were used throughout this work. The first, nonresonant Doppler-free two-photon absorption, is a standard method which has been used ex-

tensively since its first demonstration in 1974.[22,23] We have used this method to observe the $n\,^2S_{1/2}$ and $n\,^2D_{3/2,5/2}$ levels by direct absorption from the $6\,^2S_{1/2}$ ground state. A linear actively stabilized single-mode dye laser, operated with the dye DCM, provided a peak output power of 120 mW with 1-MHz linewidth in the required wavelength region. In our experimental setup (identical to Ref. 16) the laser beam was focused into the Cs cell and refocused by a second lens onto the surface of a plane mirror; thus the foci of the incident and reflected beams coincided inside the cell. Feedback into the laser was eliminated by setting the beams slightly off-axis at the lens positions and blocking the return beam at the first lens.

The second excitation scheme, resonantly enhanced Doppler-free two-photon absorption, has not previously been used for precise determination of energy levels. In this scheme the DCM laser was maintained at a fixed frequency in the Doppler profile of the $6\,^2S_{1/2}[F=4]-5\,^2D_{3/2}$ transition. This created a velocity-selected population of atoms in each of the $5\,^2D_{3/2}$ hyperfine substates ($F=2-5$) since their splittings are smaller than the Doppler widths of the individual lines. An identical second laser operated with R6G, DCM, or LD700 was tuned to the $5\,^2D_{3/2}-n\,^2P_{1/2,3/2}$, $n\,^2F_{5/2}$, or $n\,^2G_{7/2}$ transitions. The beam from this laser was arranged to pass through the Cs cell in both directions and to cross the DCM laser beam at a small angle in the center of the cell (Fig. 1). With this arrangement we observed two separate spectra which arise from the copropagating and counterpropagating laser beams. Since only linear absorption processes are involved, the beams were not focused. In fact, the power in the second laser beam was reduced for some transitions to less than 100 nW, corresponding to a power density of 3 μW/cm^2, to avoid saturation broadening. The laser beams were not expanded because our thermionic detection system required a spacially limited excitation region as provided by the crossing of small (1 mm) beams.

Two low-lying levels ($8\,^2S_{1/2}$ and $6\,^2P_{1/2}$) were determined from saturated absorption measurements on the transitions $6\,^2P_{1/2}-7\,^2D_{3/2}$, $9\,^2S_{1/2}$, $8\,^2S_{1/2}$. The $6\,^2P_{1/2}$
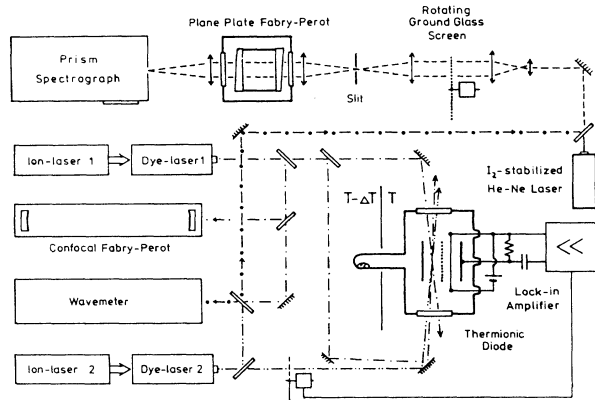
FIG. 1. Experimental apparatus for observation of Cs energy levels by resonantly enhanced two-photon absorption.

level was incidentally populated by radiative decay of $5\,^2D_{3/2}$. Since the $5\,^2D_{3/2}$ level was long lived with respect to this decay, the velocity distribution in the $6\,^2P_{1/2}$ level was collisionally smeared out and therefore suitable for saturation spectroscopy.

Detection

Atoms excited into a high-lying final state by any of the excitation schemes above were detected by using a thermionic diode system similar to that described by Harvey.[24] The electrodes were mounted inside a glass cell with optical windows and a cold finger which contained the Cs metal. The cell was prepared by baking at 720 K under a vacuum of 4×10^{-7} Torr before the Cs capsule inside was broken and the system sealed off. The body of the cell and the cold finger were placed in separately heated oven chambers with the cell at a slightly higher temperature to prevent condensation. Typical working conditions were a cathode temperature of 1000 K and a quiescent current of 30 μA. One of the lasers which illuminated the excitation region was chopped at a frequency within the 30-Hz bandwidth of the diode, and the variation of anode current was detected by a lock-in amplifier across a 10-kΩ load resistor.

For the investigation of Rydberg states, especially those with high angular momentum, elimination of stray fields is essential. There were two sources of such fields in our experiment. Small electric and magnetic fields due to the oven heating coils were eliminated by placing a grounded μ-metal shield around the detector cell. Electric fields from the detector itself were minimized by a grid at anode potential separating the filament and space charge from the excitation region. The field at the crossing point of the laser beams in the center of the excitation region was further reduced by biasing the diode to eliminate any evidence of Stark effect in the resonantly enhanced two-photon spectrum of $54\,^2G_{7/2}$, the most sensitive level observed in this experiment. Tests on this transition with and without visible asymmetry showed no detectable shift of the line peak at our level of precision. This indicates that field effects are negligible in our data.

Characteristics of the observed spectra

Our measurements of nonresonant two-photon spectra were made primarily on the $^2S_{1/2}$ and $^2D_{5/2}$ series. For S-S transitions the hyperfine structure of the states cannot be observed directly because of the $\Delta F=0$ selection rule. For S-D transitions the D-state hyperfine structure is observable at low n but becomes negligible for $^2D_{5/2}$ states with $n>12$ and $^2D_{3/2}$ states with $n>20$. The typical quality of the spectra observed is illustrated by the $6\,^2S_{1/2}[F=4]-15\,^2D_{5/2}$ transition shown in Fig. 2. For this low n transition, pressure broadening is small and the observed linewidth is only slightly over 2 MHz due entirely to the laser linewidth. At principle quantum numbers greater than 30 it becomes increasingly difficult to observe nonresonant two-photon transitions in Cs because of the onset of Cs dimer absorption which produces a strong background signal; therefore, we have not attempted to follow these series to high principal quantum numbers.

Resonant two-photon spectra show a much better signal-to-noise ratio and can be observed to very high n because the laser wavelengths required are not in the region of Cs dimer absorption. The high sensitivity obtained in this method is illustrated in Fig. 3. Here the $6\,^2S_{1/2}[F=4]-30\,^2G_{7/2}$ transition is shown in the wing of the $6\,^2S_{1/2}[F=4]-30\,^2F_{5/2}$ transition whose signal strength is greater by approximately 10^5. The $^2G_{7/2}$ series is excited by a resonant double electric quadrupole process and is readily observed to $n=50$. For higher n observation is difficult because of the close proximity of the much stronger $^2F_{5/2}$ transitions.

The general characteristics of the resonantly enhanced two-photon spectra are shown in Fig. 4. The spectrum was recorded with both copropagating and counterpropagating beams present. The laser tuned to the $6S$-$5D$ transition was held at a fixed wave number σ_1 close to the
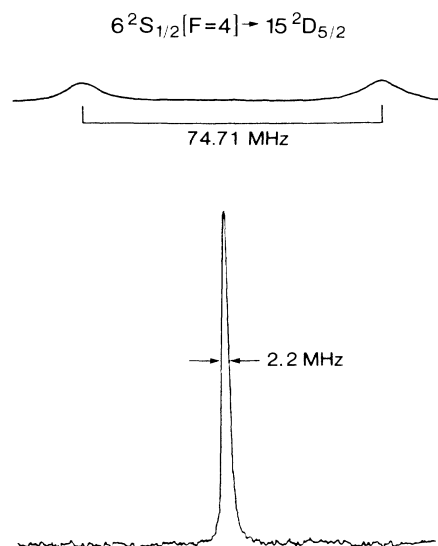
$$6\,^2S_{1/2}[F=4] \rightarrow 15\,^2D_{5/2}$$

FIG. 2. Scan of the Cs two-photon transition $6\,^2S_{1/2}[F=4]-15\,^2D_{5/2}$. The frequency scale is calibrated by the simultaneously recorded transmission of a confocal Fabry-Perot interferometer.
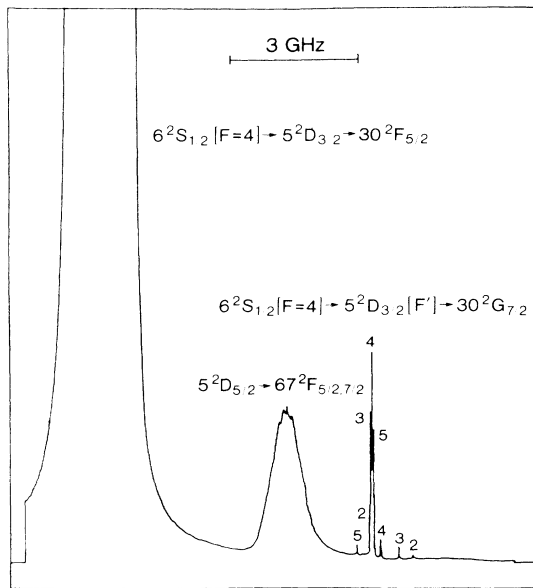
FIG. 3. Scan showing the $6\,^2S_{1/2}\rightarrow 5\,^2D_{3/2}\rightarrow 30\,^2G_{7/2}$ resonantly enhanced two-photon transition in the wing of the $6\,^2S_{1/2}\rightarrow 5\,^2D_{3/2}\rightarrow 30\,^2F_{5/2}$ transition which is stronger by a factor of 10^5. The lines are coincidentally adjacent to a Doppler-limited absorption from the collisionally populated $5\,^2D_{5/2}$ level.

center of the Doppler profile while the second laser wave number σ_2 was scanned across the $5D$-$26G$ transition. The multiple resonances observed in the spectrum are due to the hyperfine structure of the intermediate $5\,^2D_{3/2}$ level. The splitting of $5\,^2D_{3/2}$ appears expanded by a factor of $(\sigma_1+\sigma_2)/\sigma_1$ in the spectrum originating from the copropagating beams and contracted by $(\sigma_1-\sigma_2)/\sigma_1$ in the counterpropagating spectrum. For the case shown
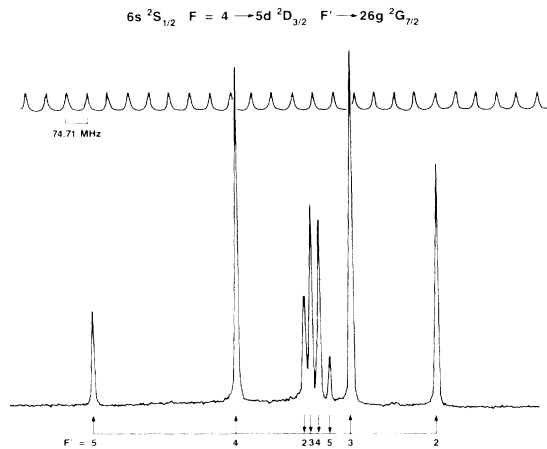
$\sigma_1 < \sigma_2$, hence the hyperfine components appear in reversed order in the counterpropagating spectrum. We have chosen to use the $5D$ level with $J = \frac{3}{2}$ as our intermediate state because its wider hyperfine intervals are more easily resolved in the contracted spectrum. This is an important consideration at low n where σ_1 and σ_2 can be nearly equal.

In Fig. 5 we show the $6\,^2S_{1/2}[F=4]-9\,^2P_{1/2}$ transition as a final example of the resonant two-photon method. The complexity of the spectrum is due to the resolved hyperfine structure of the $9\,^2P_{1/2}$ level in addition to the structure of the intermediate state. The origin of each of the components is indicated in the figure. Only the intervals of the intermediate-state structure are altered by Doppler shifts in the recorded spectra. The hyperfine structure of the final state appears with its correct intervals in both the copropagating and counterpropagating spectra. The very weak components visible in this spectrum are caused by collisionally induced transitions between hyperfine levels of the intermediate state. Since these low-energy collisions do not significantly change the velocities of the excited atoms, weak Doppler-free ghosts can occur at the hyperfine intervals from the regular resonances.

In Figs. 3—5 the relative intensities of the copropagating and counterpropagating spectra are arbitrarily determined by the beam alignments and the power densities in the crossing volume. The intensity ratios of the hyperfine structure components reflect a convolution of the transition probabilities with the individual component Doppler profiles at the $6S$-$5D$ laser wave number.

In all of our resonant two-photon spectra linewidths of 3—7 MHz were observed. Of this 2 MHz can be attributed to the combined laser bandwidths and as much as 5 MHz to the residual Doppler broadening from the $<0.5°$ crossing angle of the beams in the detector. The third significant broadening mechanism is intrinsic pressure broadening. For a particle density of 2×10^{13} cm^{-3} this mechanism produces a final-state level width which

FIG. 4. Scan of the $6\,^2S_{1/2}\rightarrow 5\,^2D_{3/2}\rightarrow 26\,^2G_{7/2}$ double quadrupole transition showing the typical characteristics of our resonantly enhanced two-photon spectra. The resonances due to copropagating beams are identified with erect arrows and those due to counterpropagating beams with inverted arrows.
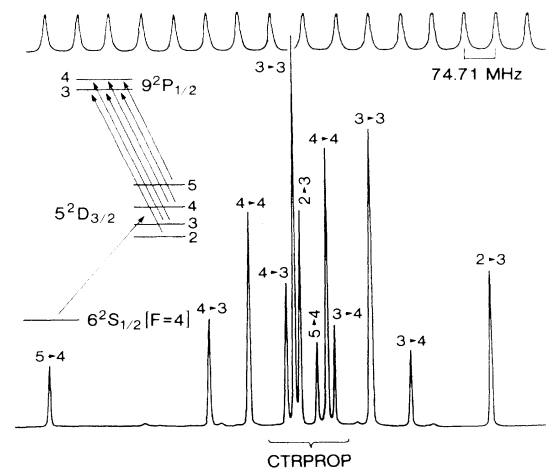

FIG. 5. Scan of the $6\,^2S_{1/2}\rightarrow 5\,^2D_{3/2}\rightarrow 9\,^2P_{1/2}$ transition showing the resolved hyperfine structure of the $9\,^2P_{1/2}$ level.

ranges from negligible for low n to 4 MHz for Rydberg states. Because of the unfocused beams and low power densities used in this experiment, transit and saturation broadening were negligible. The natural width of the intermediate state which should cause slightly broader lines in the copropagating spectrum than in the counterpropagating spectrum was also undetectable.

Absolute energy measurements

In nonresonant two-photon spectroscopy the energy of an observed level is simply twice the laser wave number since the experimental method inherently provides for the cancellation of first-order Doppler effects. In resonantly enhanced two-photon spectroscopy it is necessary to provide explicitly for elimination of Doppler shifts in the measurement technique.

A narrow-band laser tuned into the Doppler profile of a transition i-k populates a class of atoms in the upper state k with velocity

$$v = (\sigma_1/\sigma_{10} - 1)c$$

parallel to the laser beam, where σ_1 and σ_{10} are the wave numbers of the laser light and of the unshifted atomic transition, respectively, and c is the velocity of light. A second laser with wave number σ_2 can excite these atoms to a final state f if the condition

$$\sigma_2 = \sigma_{20}(1 \pm v/c)$$

is fulfilled. Here the $+$ sign refers to copropagating, and the $-$ sign to counterpropagating, laser beams. Since the atomic transition wave numbers are defined by

$$\sigma_{10} = E_k - E_i \; ,$$

$$\sigma_{20} = E_f - E_k \; ,$$

in the special case where the lasers are tuned to σ_{10} and σ_{20} the energy of the final state with respect to the initial state is the sum of the laser wave numbers. This special case cannot be readily realized experimentally.

In the general case where the velocity component of the atoms along the direction of the laser beams does not vanish, the sum of the laser wave numbers is offset from desired energy interval by

$$E_f - E_i = \sigma_{10} + \sigma_{20} = (\sigma_1^\pm + \sigma_2^\pm) - (\sigma_{10} \pm \sigma_{20})v/c \; ,$$

where the signs again refer to the copropagating and counterpropagating beams. A set of the four wave numbers σ_1^+, σ_1^-, σ_2^+, and σ_2^- is sufficient to eliminate the velocity from the equations and determine the wave numbers of the atomic transitions

$$\sigma_{10} = (\sigma_1^+ \sigma_2^- / \sigma_2^+ + \sigma_1^-)/2 \; ,$$

$$\sigma_{20} = (\sigma_2^+ \sigma_1^- / \sigma_1^+ + \sigma_2^-)/2 \; .$$

The energy of the final state is then

$$E_f = E_i + \sigma_{10} + \sigma_{20} = E_k + \sigma_{20} \; .$$

Experimentally this means that one must measure the wave numbers of the two dye lasers tuned to the same resonance in both the copropagating and counterpropagating

spectra. Each such set of wave numbers provides an independent measurement of both the intermediate- and final-state energies.

Measurement of laser wave numbers

Because of the high resolution and excellent signal-to-noise ratio in our observed spectra, it was possible to tune our lasers to the peak of a two-photon resonance with an uncertainty of less than 2 MHz. To fully utilize this accuracy in the determination of absolute energy levels it was necessary to make precise measurements of the laser wave numbers. Consequently we carried out our measurements in two steps. As shown in Fig. 1, a small fraction of the intensity was taken from each of the laser beams, and these two weak beams were combined on a beam-splitter to provide collinear beams in two directions. One of these was directed to an air-track Michelson-type wavemeter which, with fringe multiplication, provided a resolution of 0.000 13 cm^{-1}. A commercial frequency-stabilized He-Ne laser was used for a reference. The wavemeter was calibrated using optogalvanic lines of Th and U (Ref. 25) and had an experimentally determined uncertainty (95% confidence) of 0.0008 cm^{-1} for a single measurement. The two dye-laser wave numbers were measured sequentially by blocking one or the other of the beams.

The final determination of the laser wave numbers was made by classical Fabry-Perot interferometry.[16,26] The collinear dye-laser beams were combined with the output of an iodine-stabilized He-Ne laser locked to hyperfine component g of the $^{127}I_2$ transition $R(127)$ 11-5. The wave number produced by this laser, 15 798.007 183(16) cm^{-1}, is an internationally accepted realization of the definition of the meter.[27] The three combined beams were expanded and scattered from a rotating ground glass screen which served as an extended light source for illumination of the interferometer. The fringe patterns were focused on the slit of a prism spectrograph and photographed. By this method both dye lasers were measured simultaneously and the length of the interferometer spacer was redetermined with respect to an accepted standard for every measurement. For all measurements in this work a 218-mm evacuated interferometer was used. With each set of data the integer order of interference for the reference laser was checked using optogalvanic lines of U and Th calibrated for this purpose.[25] Integer order numbers for the dye lasers were determined unambiguously from the initial wavemeter measurements. Finally, computer analysis of the photographically recorded fringe patterns determined the fractional order of interference to better than 0.003 order corresponding to a wave-number uncertainty of 0.000 07 cm^{-1}.

The only known source of systematic error in the wave-number measurements which may be significant at our level of accuracy is the wavelength-dependent phase shift on reflection from the interferometer coatings. In previous work in this laboratory it has been shown that the size of this effect is 0.000$\pm$0.003 order throughout the wavelength region of interest. Our data has not been corrected for this effect which may produce a maximum error of 0.000 07 cm^{-1}.

RESULTS

Energy levels determined for the five Cs series in which we have made extensive observations are presented in Table I. A few levels of two other series have also been determined and are given in Table II. All of the levels have been corrected to remove the effects of hyperfine structure and pressure shifts and represent the center-of-

TABLE I. Energy levels of Cs series for which extensive observations were made in this work. Units are cm^{-1}. All energies refer to the centers of gravity of both the ground and excited levels and have been corrected for pressure shifts as described in the text. The uncertainty (95% confidence) in the levels is 0.000 15 cm^{-1} for the p, f, and g series and 0.000 20 cm^{-1} for the s and d series except where a different uncertainty is explicitly stated in parentheses.

n	$^2S_{1/2}$	$^2P_{1/2}$	$^2D_{5/2}$	$^2F_{5/2}$	$^2G_{7/2}$
5			14 596.842 32		
6	00 000.0000(0)	11 178.2686(5)		28 329.5133(5)	28 352.4444(5)
7			26 068.7730(5)	29 147.981 88	29 163.072 06
8	24 317.1500(5)		27 822.8802(5)	29 678.742 80	29 689.137 95
9	26 910.6627(5)	27 636.9966(5)	28 835.791 92	30 042.314 05	30 049.753 17
10	28 300.2287(5)	28 726.8123(5)	29 472.939 95	30 302.165 37	30 307.660 76
11	29 131.730 04	29 403.423 10	29 899.546 46	30 494.288 09	30 498.456 95
12	29 668.803 36	29 852.431 53	30 199.098 21	30 640.320 28	30 643.554 84
13	30 035.788 36	30 165.668 26	30 417.460 75	30 753.904 06	30 756.462 41
14	30 297.645 10	30 392.871 83	30 581.527 58	30 843.984 88	30 846.042 23
15	30 491.023 46	30 562.908 93	30 707.913 78	30 916.625 83	30 918.304 48
16	30 637.882 76	30 693.474 16	30 807.332 97	30 976.053 85	30 977.440 90
17	30 752.034 12	30 795.907 02	30 886.945 13	31 025.289 07	31 026.448 32
18	30 842.517 75	30 877.747 61	30 951.682 59	31 066.535 82	31 067.514 35
19	30 915.452 62	30 944.168 59	31 005.032 31	31 101.433 21	
20	30 975.100 34		31 049.517 01	31 131.220 12	31 131.935 70
21	31 024.503 55	31 044.313 15	31 086.997 17		
22	31 065.880 56		31 118.869 83	31 179.056 92	31 179.595 67
23	31 100.880 52	31 115.117 33	31 146.200 07		
24	31 130.749 87		31 169.811 87	31 215.426 20	31 215.841 76
25	31 156.444 39	31 167.017 27	31 190.350 63		
26	31 178.707 60		31 208.327 04	31 243.720 69	31 244.048 16
27	31 198.124 16	31 206.189 67			
28	31 215.159 66		31 238.151 45	31 266.164 99	31 266.427 36
29	31 230.188 05	31 236.480 30			
30	31 243.512 52		31 261.715 76	31 284.267 68	31 284.481 10
31	31 260.384 52				
32			31 280.656 87	31 299.079 98	31 299.255 84
33		31 279.579 37		31 305.495 90	
34			31 296.109 80		31 311.500 61
35				31 316.716 03	
36		31 301.984 46	31 308.881 06	31 321.637 42	31 321.761 08
37		31 308.145 96			
38				31 330.339 31	31 330.444 63
40		31 323.681 94			
41				31 341.080 65	
42		31 332.079 13			31 344.237 86
44		31 339.260 62		31 349.699 35	31 349.767 27
46					31 354.591 16
47		31 348.229 38		31 356.719 91	
50		31 355.515 63		31 362.514 22	31 362.560 44
53		31 361.515 23		31 367.352 41	
54					31 368.824 92
56		31 366.514 31		31 371.433 26	
59		31 370.723 68		31 374.907 59	
62		31 374.301 13		31 377.889 40	
65		31 377.367 25		31 380.467 77	
68		31 380.015 00			
71		31 382.317 24			
74		31 384.333 30			
77		31 386.103 63			
80		31 387.671 44			

TABLE II. Energies of additional Cs levels observed in this work. Units are cm^{-1}.

Series	n	Energy[a]
$^2P_{3/2}$	18	30 880.122 87
	25	31 167.742 47
	33	31 279.859 34
	44	31 339.368 76
$^2D_{3/2}$	5	14 499.258 37
	7	26 047.845 8(5)
	9	28 828.678 75
	10	29 468.284 46
	11	29 896.336 64
	13	30 415.749 92
	19	31 004.588 85

[a]All energies refer to the centers of gravity of both the ground and excited levels and have been corrected for pressure shifts as described in the text. The estimated uncertainty (95% confidence) is 0.000 20 cm^{-1} except where a different uncertainty is explicitly stated in parentheses.

gravity energies of the unperturbed atom.

For correction of the measured energies to the centers of gravity of the ground and excited levels, we have used published data on hyperfine splittings and some new hyperfine intervals determined in this work. All of our experimental observations were made with respect to the $F = 4$ component of $6 {}^2S_{1/2}$ and have been increased by 0.134 15 cm^{-1} to correct for the ground-state structure. Since the hyperfine structure of the $n {}^2S_{1/2}$ states is not directly observable, a formula was fit to intervals drawn from the literature[28−31] and used for correction of the excited level structure. For the $n {}^2P_{1/2}$ levels literature values[31−36] were combined with our measurements of a few intervals (given in Table III) to produce a similar formula.[37] For this series the excited-state hyperfine correction is negligible for $n > 40$. Final-state hyperfine corrections were negligible for most $^2D_{5/2}$ and all $^2F_{5/2}$ and $^2G_{7/2}$ states. For a few low-lying $^2D_{3/2}$ levels all resolved hyperfine components were measured and used to determine the center of gravity.

The experimentally determined energy levels have also been adjusted to correct for intrinsic pressure shifts. Although these shifts are smaller than the statistical uncertainties, they are a significant systematic offset, especially for levels with large n. Extensive investigations of collisional shifts in alkali-metal Rydberg levels (Ref. 38 and references therein) have shown that, in the range of particle densities applicable to this work, the level shift δ de-

TABLE III. Cs I $^2P_{1/2}$ hyperfine-structure intervals measured in this work.

n	$^2P_{1/2}[F = 4] - {}^2P_{1/2}[F = 3]$ (MHz)
11	35.5(1.0)
12	23.1(1.0)
13	17.1(1.0)
14	15.2(2.0)
15	10.3(1.0)

pends linearly on the particle density N. Shift coefficients δ/N have been determined for Cs D levels up to quantum numbers n where they become constant with respect to all parameters except the kind of perturber. This maximum shift coefficient is the same for all levels with $n > 35$ independent of n and the angular momentum l. Levels with $n < 35$ behave similarly for different l except for non-monotonic variations with n which cause deviation of up to 40% from the smooth overall dependence. Whether such nonmonotonic features are present in the pressure shift for S, P, F, or G levels of Cs is not known.

To correct for pressure shift the Cs particle density in our thermionic diode was determined by two methods. Initially we measured the equivalent width of the resonance line in absorption as described in Ref. 38 at somewhat higher temperatures than used in our experiment and extrapolated to our conditions using the Cs vapor pressure curve. Later the width of the $6S$-$20S$ two-photon line was measured for different diode temperatures, and the known self-broadening coefficient was used to determine the particle density. The two results agree within 15%, well within the combined uncertainties, and yield a Cs particle density of 2×10^{13} cm^{-3} for the oven temperature typically used for our energy-level measurements. For this density the maximum correction applied to all levels with $n > 35$ is $+ 0.000 08$ cm^{-1}. At lower n the uncertainty in the shift correction due to nonmonotonic variation with n does not exceed 0.000 03 cm^{-1}.

As a final check on our pressure-shift correction, we measured a few strong transitions at a much lower particle density estimated to be 3×10^{12} cm^{-3}. For this density, pressure shifts should be negligible. The levels measured at low density were in good agreement with our other pressure corrected data. This validates the correction made for pressure shift.

ANALYSIS

The energy levels of the five Cs series we have observed can be represented with high precision by the modified Ritz formula

$$E_n = E_\infty - R/(n - \mu_n)^2 ,$$

where E_n is the energy of the level with principal quantum number n, E_∞ is the ionization limit, R is the Rydberg constant (109 736.862 24 cm^{-1} for ^{133}Cs), and μ_n is the quantum defect given by the expansion

$$\mu_n = A + B/(n - A)^2 + C/(n - A)^4 + \cdots .$$

By using a nonlinear least-squares-fitting routine, the ionization limit and expansion parameters were simultaneously optimized for each series using an increasing number of terms in the expansion until all energy levels were represented within their uncertainties and the residuals E_n(calc) $- E_n$(expt) were randomly distributed.

In order to determine series formulas applicable to all n, we have used experimental energies from other sources for a few low-lying levels not observed in this work. These additional data, which are given in Table IV, were included in our fitting with reduced weights appropriate to their greater uncertainties. The resulting formulas are

TABLE IV. Data from other sources used in fitting series formulas. Units are cm^{-1}.

Series	n	Energy[a]	Footnote
$^2S_{1/2}$	7	18 535.5286(30)	b
$^2P_{1/2}$	7	21 765.348(20)	c
	8	25 708.833(30)	d
$^2D_{3/2}$	6	22 631.6863(10)	e
$^2F_{7/2}$	4	24 472.2269(20)	f
	5	26 971.3030(30)	f
$^2G_{7/2}$	5	27 008.0541(20)	g

[a]The uncertainty cited has, in some cases, been increased from that reported in the original source to reflect the judgement of the current authors.
[b]Weighted average based on seven infrared transitions measured by Johansson (Ref. 3) and by Sansonetti (unpublished) combined with the $7p$ level values of Kleiman (Ref. 4) and the $8\,^2P_{1/2}$ level of this work.
[c]Reference 4.
[d]Weighted average based on six transitions measured by Kleiman (Ref. 4) and by Sansonetti (unpublished) combined with s and d levels from this work.
[e]Reference 5.
[f]Reference 6.
[g]Reference 8.

FIG. 6. Deviations of our experimentally determined energy levels from the modified Ritz formulas of Table V.

summarized in Table V and the residuals for the levels measured in this work are plotted in Fig. 6. The ionization limits for all five series agree within an interval of only 0.000 05 cm^{-1}. The residuals for 96% of the levels measured in this work do not exceed 0.000 15 cm^{-1}.

The same data have also been fitted with the extended Ritz formula in which μ_n is expanded in inverse even powers of $(n - \mu_n)$. The data are represented equally well by the extended formula and in no case is there a statistically significant variation in the calculated ionization limit. We have chosen to report the results for the modified formula only because of its convenience for calculation.

The polarization formula provides an alternative means for representing a series of energy levels if the external electron is nonpenetrating. In this case the deviation of the energy levels from their hydrogenic positions is due almost entirely to the polarization of the ion core in the field of the external electron and the energy can be written
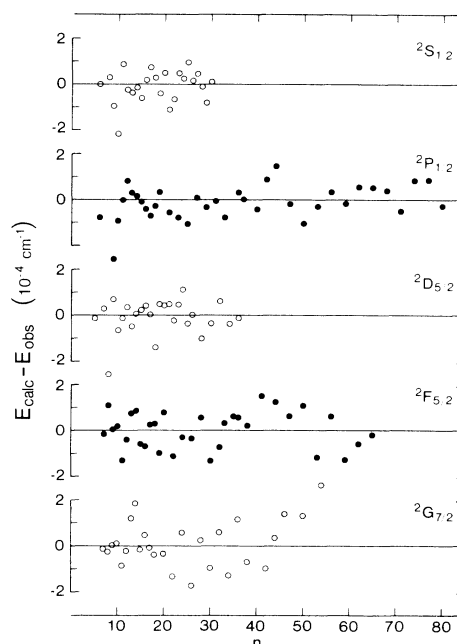
as

$$E_n = E_\infty - T_H(n,l) - Ra_0[\alpha'_d \langle r^{-4}(n,l) \rangle + \alpha'_q \langle r^{-6}(n,l) \rangle] \, ,$$

where α'_d and α'_q are the effective dipole and quadrupole polarizabilities of the core, a_0 is the Bohr radius, and the expectation values $\langle r^{-4} \rangle$ and $\langle r^{-6} \rangle$ are to be determined for the appropriate hydrogenic state.[39] The relativistic hydrogenic term value is given by

$$T_H(n,l) = \frac{R}{n^2} \left[1 + \frac{\alpha^2}{n^2} \left[\frac{n}{l+1/2} - \frac{3}{4} \right] \right] \, ,$$

where α is the fine-structure constant. The polarization formula does not include fine-structure splitting but can be applied to the centers of gravity of the doublet terms of an alkali-metal atom such as Cs.

The polarization formula was used by Bockasten[40] and by Sansonetti, Andrew, and Verges[8] to represent the ^2F

TABLE V. Ionization limits and quantum defect expansion coefficients for Cs I series measured in this work. The uncertainties given in parentheses for E_∞ and A are the asymptotic standard deviations of the parameters determined by the nonlinear least-squares-fitting algorithm.

	$n\,^2S_{1/2}$ ($n=6-30$)	$n\,^2P_{1/2}$ ($n=6-80$)	$n\,^2D_{5/2}$ ($n=5-36$)	$n\,^2F_{5/2}$ ($n=4-65$)	$n\,^2G_{7/2}$ ($n=5-50$)
E_∞	31 406.467 69(2)	31 406.467 65(2)	31 406.467 67(3)	31 406.467 66(2)	31 406.467 64(3)
A	4.049 356 65(38)	3.591 589 50(58)	2.466 315 24(63)	0.033 414 24(96)	0.007 038 65(70)
B	0.237 703 7	0.360 926	0.013 577	$-0.198\,674$	$-0.049\,252$
C	0.255 401	0.419 05	$-0.374\,57$	0.289 53	0.012 91
D	0.003 78	0.643 88	-2.1867	-0.2601	
E	0.254 86	1.450 35	-1.5532		
F			-56.6739		

and ^2G series of cesium. The latter authors attempted to calculate the nonpolarization contributions to the ^2F terms and concluded that up to 20% of the term defect for this series was not due to polarization. Nevertheless, the polarization formula gave an excellent description of the experimental data.

Using the more extensive and accurate data from this work, we have made new fits of the polarization formula to these series. For the ^2G series we have approximated the doublet centers of gravity using the hydrogenic ^2G splitting[41] since the fine structure was found to be very nearly hydrogenic in Ref. 8. For the ^2F series we have used the fine-structure intervals of Ref. 21 to determine the centers of gravity. We find that the ^2G series is described within the uncertainty of the data by a polarization formula with $E_\infty = 31\,406.467\,68(2)$ cm^{-1}, $\alpha'_d = 15.770(3)a_0^3$, and $\alpha'_q = 48.9(4)a_0^5$. Here the uncertainties given in parentheses are the asymptotic standard deviations of the parameters as determined by the nonlinear least-squares-fitting algorithm. The ^2F series, however, cannot be adequately represented by the polarization formula. Even when the lowest three members of the series are excluded from the fit, systematic deviations of the order of 0.0004 cm^{-1} are apparent in the residuals.

DISCUSSION

Our results for all series observed in this work can be compared directly with previously published data. Comprehensive Doppler-free measurements of the $^2S_{1/2}$ and $^2D_{5/2}$ series have been reported by O'Sullivan and Stoicheff[12] and by Lorenzen and Niemax[11] in experiments very similar to ours except for the use of traveling-mirror Michelson wavemeters to determine the laser wavelength. The differences of their energies from the data of this work are shown in Fig. 7. The results of O'Sullivan and Stoicheff display a large scatter with an average systematic offset of about -0.005 cm^{-1} over this range of n. The data of Lorenzen and Niemax[42] show much better internal consistency but are offset from our results by $+0.0034(3)$ cm^{-1} which is substantially outside the combined uncertainties.

Doppler-limited absorption measurements of the $^2P_{1/2}$ series using a frequency-doubled dye laser have also been reported by Lorenzen and Niemax.[11] Comparison of their measured data with our results for this series again shows a systematic offset of $+0.0029(11)$ cm^{-1} in agreement with the offset for the ^2S and ^2D series.

All of the measurements of Lorenzen and Niemax were made with respect to a commercial frequency-stabilized He-Ne laser whose wavelength was determined using a set of Doppler-free reference lines in Rb as proposed by Lee, Helmcke, Hall, and Stoicheff.[14] To determine whether the discrepancies in the Cs results could be traced to the reference lines, we have made additional measurements in Rb which have been reported elsewhere.[16] Although small differences from the results of Lee et al. were found, these differences do not account for the Cs deviations.

We cannot explain the systematic offset between our results and those of Lorenzen and Niemax, but it seems very
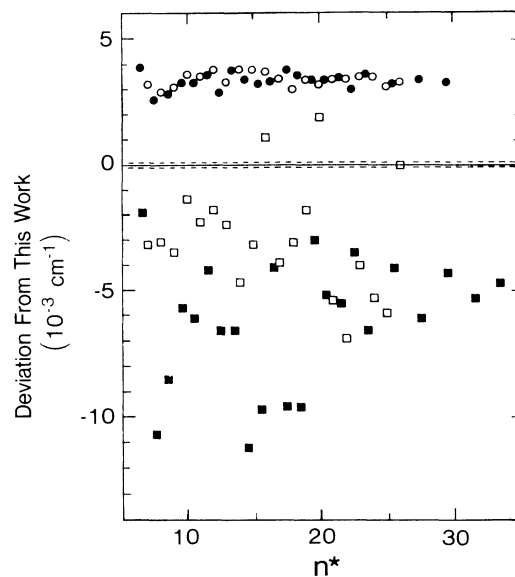

FIG. 7. Deviations between previously reported data and the $^2S_{1/2}$ (open symbols) and $^2D_{1/2}$ (solid symbols) levels of Table I. Squares: O'Sullivan and Stoicheff (Ref. 12). Circles: Lorenzen and Niemax (Ref. 11). The dashed lines indicate the uncertainty of our results.

likely that it stems from the laser wavelength measurement rather than from any shift of the atomic levels. It is interesting to note that the earlier measurements of Lorenzen, Weber, and Niemax[9] for the ^2S and ^2D series, despite their large scatter, show no systematic deviation from our data. For these measurements the laser wavelength was determined from the molecular iodine spectrum rather than by use of a wavemeter.

The accuracy of our Fabry-Perot wavelength measurements over a narrow wavelength range in the vicinity of 6100 Å has been demonstrated in our previous work.[16] The excellent agreement of the ionization limits derived from the five series measured in this work (Table V) gives strong evidence that there is no wavelength-dependent error in our measurements. For the even-parity series observed by nonresonant two-photon absorption, the laser wavelength was about 6390 Å for the levels with highest n. For the odd-parity states observed by resonantly enhanced two-photon absorption, the two lasers were tuned to 6895 and about 5920 Å. It is very unlikely that the series would give the same limit using such different wavelengths if a wavelength-dependent error were present in the measurement technique.

No previous measurements of the ^2F and ^2G series using laser techniques have been reported; however, energies of low members of these series have been determined using classical emission measurements. The best values for the ^2F series were given by Eriksson and Wenåker[6] using a hollow-cathode discharge and grating spectrograph. Energies for the ^2G series were given by Sansonetti, Andrew, and Verges[8] using a pulsed radio-frequency discharge and Fourier spectrometer. For both of these experiments the uncertainty of the energy levels was estimated to be 0.001

cm^{-1}. Results from these experiments are compared with our current data in Fig. 8. The similarity of the deviations for these two series measured with different types of sources in independent experiments is striking. For both series the emission results give lower energies than our current data with deviations that increase with increasing n. Apparently field and pressure shifts in the discharge sources were much larger than estimated by the experimenters based on the profiles of the emission lines.

Our data can also be compared with the precise measurements of microwave transitions among Cs Rydberg states made by Goy et al.[30] For this comparison we have used the series formulas from Table V to calculate the relevant microwave transition frequencies. For the 16 $n\,^2S_{1/2}-(n+1)\,^2S_{1/2}$ and $n\,^2D_{5/2}-(n+1)\,^2D_{5/2}$ two-photon transitions measured by Goy et al., the agreement is excellent. All deviations are less than 1 MHz and the standard deviation of the two sets of values is 0.26 MHz. For ten $n\,^2S_{1/2}-n\,^2P_{1/2}$ transitions the agreement is also very good. Only the results for $n=34$ and 42 differ by more than the stated uncertainty of the microwave measurements, and these two values also failed to agree with the formulas of Goy et al.

Agreement for the $n\,^2D_{5/2}-(n-3)\,^2F_{5/2}$ transitions is somewhat less satisfactory. In particular, for $32D$-$29F$ the deviation is 8.5 MHz and for $33D$-$30F$ it is 10.5 MHz with the measured frequency higher than predicted by our formulas. Since the ionization limits derived from our $^2D_{5/2}$ and $^2F_{5/2}$ series agree within 1 MHz, it seems unlikely that these deviations arise from errors in the formulas. The direction of the deviation is consistent with Stark shifts in the microwave data. Goy et al. estimated that

electric fields of 100 mV/cm existed in their apparatus and suggested that Stark effect might be responsible for discrepancies in their data at high n.[30]

A few additional microwave measurements of $n\,^2F-n\,^2G$ ($n=15-17$) transitions in Cs have been reported by Ruff, Safinya, and Gallagher.[43] Although the estimated uncertainty of the measurements was 1—4 MHz, the results disagree with our predictions by 32.8 MHz at $n=15$, 9.8 MHz at $n=16$, and 10.2 MHz at $n=17$. In the experiment of Ruff et al., Cs atoms were prepared in a $n\,^2F$ state by two-step laser excitation, the first step being the $6\,^2S_{1/2}-7\,^2P_{3/2}$ transition at 4556 Å. Recently it has been shown by McIlrath et al.[44] that low-pressure Cs vapor is efficiently photoionized by pumping on the $6\,^2S_{1/2}-7\,^2P_{3/2}$ transition at 4593 Å. The 4556-Å line has a higher transition probability and is probably even more efficient for the ionization process. It seems likely, therefore, that many Cs ions and free electrons were present in the measurements of Ruff et al. and that the presence of these charged species was the cause of the unexplained line broadening observed. The direction of the deviations between the measured transition frequencies and our predictions is consistent with Stark shifts in the microwave data.

All of the best data for the series observed in this work are summarized graphically in Fig. 9 where we have plotted the quantum defects for each series versus n. The $^2S_{1/2}$ and $^2P_{1/2}$ quantum defects fall on smooth asymptotically decreasing curves characteristic of series for which the penetration of the core by the valence electron is the primary contributor to the term defects. For such a series the core potential has little dependence on n of the
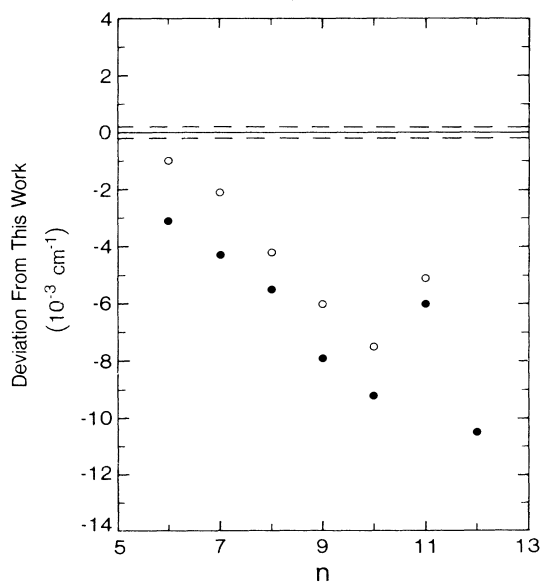

FIG. 8. Deviations between previously reported data and the $^2F_{5/2}$ and $^2G_{7/2}$ levels of Table I. Solid circles: $^2F_{5/2}$ from Eriksson and Wenåker (Ref. 6). Open circles: $^2G_{7/2}$ from Sansonetti, Andrew, and Verges (Ref. 8). The dashed lines indicate the uncertainty of our results.
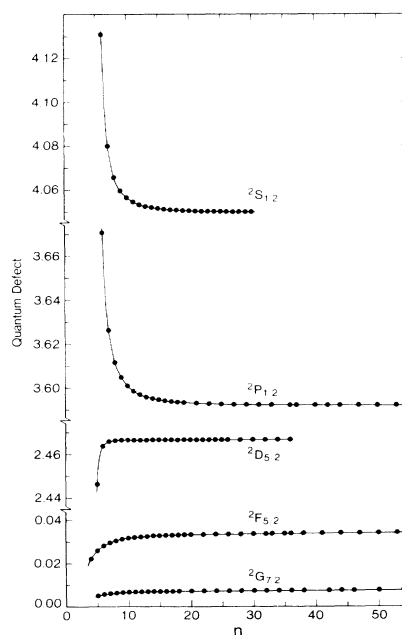

FIG. 9. Experimental quantum defects for all Cs series observed in this work.

valence electron. The $^2F_{5/2}$ and $^2G_{7/2}$ series show a smooth asymptotically increasing variation of quantum defect because the term defects for these series are dominated by the polarization of the core in the field of the nonpenetrating valence electron. The $^2D_{5/2}$ quantum defect curve, however, increases rapidly at low n, changes slope dramatically between $n = 6$ and 7, reaches a maximum at $n = 10$, and has a slight asymptotic decrease for $n > 10$.

The unusual behavior of the ^2D quantum defect was noted by Lorenzen and Niemax.[10] In a later paper they suggested that this behavior resulted from competition between polarization and penetration effects.[11] Using the polarization formula to estimate the polarization contribution to the term defect for low members of the ^2D series, we find that it could account for only about 10% of the term defect. The external d electron is strongly penetrating, and it is most unlikely that polarization could dominate the low n dependence. It is more likely that the rise of the quantum defect at low n results from a strong core relaxation effect.

CONCLUSIONS

We have made precise new measurements of the energies of the $^2S_{1/2}$, $^2P_{1/2}$, $^2D_{5/2}$, $^2F_{5/2}$, and $^2G_{7/2}$ levels of Cs over a wide range of principal quantum numbers. Modified Ritz formulas fit to these series (Table V) permit the calculation of the level values to an accuracy better than that of any single measurement. Using fine-structure data from Refs. 21 and 30 in conjunction with these formulas permits calculation of the $^2P_{3/2}$, $^2D_{3/2}$, and $^2F_{7/2}$ levels with similar accuracy. The location of levels with higher angular momentum can be estimated using the polarization formula with effective dipole and quadrupole polarizabilities determined from our ^2G data.

The internal consistency of our data is demonstrated by the excellent agreement of the Cs ionization energies derived separately from each of our five series. All five values (Table V) lie within an interval of 0.000 05 cm^{-1}. When we take account of possible systematic errors in the laser wavelength measurements or due to pressure and Stark shifts, we find the Cs ionization energy with respect to the $6\,^2S_{1/2}$ ground-state center of gravity to be 31 406.467 66(15) cm^{-1}.

Note added in proof: At the time this manuscript was submitted for publication we were unaware of a previous precise determination of the energy of the $8\,^2S_{1/2}$ level [P. P. Herrmann, J. Hoffnagle, A. Pedroni, N. Schlumpf, and A. Weis, Opt. Commun. **56**, 22 (1985)]. The result of Herrmann *et al.*, $E(8\,^2S_{1/2}) = 24\,317.1499(4)$ cm^{-1}, is in agreement with our value, 24 317.1500(5) cm^{-1}, reported in Table I.

*Present address: MBB-ERNO Space Technology, Dept. RA 321, Hüneseld Str. 1-5, 2800 Bremen 1, Federal Republic of Germany.

[1]H. R. Kratz, Phys. Rev. **75**, 1844 (1949).

[2]J. R. McNally, Jr., J. P. Molnar, W. J. Hitchcock, and N. F. Oliver, J. Opt. Soc. Am. **39**, 57 (1949).

[3]I. Johansson, Ark. Fys. **20**, 135 (1961).

[4]H. Kleiman, J. Opt. Soc. Am. **52**, 441 (1962).

[5]K. B. Eriksson, I. Johansson, and G. Norlén, Ark. Fys. **28**, 233 (1964).

[6]K. B. S. Eriksson and I. Wenåker, Phys. Scr. **1**, 21 (1970).

[7]C.-J. Lorenzen and K. Niemax, J. Quant. Spectrosc. Radiat. Transfer **22**, 247 (1979).

[8]C. J. Sansonetti, K. L. Andrew, and J. Verges, J. Opt. Soc. Am. **71**, 423 (1981).

[9]C.-J. Lorenzen, K.-H. Weber, and K. Niemax, Opt. Commun. **33**, 271 (1980).

[10]C.-J. Lorenzen and K. Niemax, Z. Phys. A **311**, 249 (1983).

[11]C.-J. Lorenzen and K. Niemax, Z. Phys. A **315**, 127 (1984).

[12]M. S. O'Sullivan and B. P. Stoicheff, Can. J. Phys. **61**, 940 (1983).

[13]G. Avila, P. Gain, E. de Clercq, P. Cerez, Metrologia **22**, 11 (1986).

[14]S. A. Lee, J. Helmcke, J. L. Hall, and B. P. Stoicheff, Opt. Lett. **3**, 141 (1978).

[15]B. P. Stoicheff and E. Weinberger, Can. J. Phys. **57**, 2143 (1979).

[16]C. J. Sansonetti and K.-H. Weber, J. Opt. Soc. Am. B **2**, 1385 (1985).

[17]C.-J. Lorenzen, K. Niemax, and L. R. Pendrill, Opt. Commun. **39**, 370 (1981).

[18]F. V. Kowalski, K. Niemax, and L. R. Pendrill (unpublished).

[19]J. E. Bjorkholm and P. F. Liao, Phys. Rev. A **14**, 751 (1976).

[20]P. F. Liao and J. E. Bjorkholm, Phys. Rev. Lett. **36**, 1543 (1976).

[21]C. J. Sansonetti and C.-J. Lorenzen, Phys. Rev. A **30**, 1805 (1984).

[22]F. Biraben, B. Cagnac, and G. Grynberg, Phys. Rev. Lett. **32**, 643 (1974).

[23]M. D. Levenson and N. Bloembergen, Phys. Rev. Lett. **32**, 645 (1974).

[24]K. C. Harvey, Rev. Sci. Instrum. **52**, 204 (1981).

[25]C. J. Sansonetti and K.-H. Weber, J. Opt. Soc. Am. B **1**, 361 (1984).

[26]K. W. Meissner, J. Opt. Soc. Am. **31**, 405 (1941).

[27]Metrologia **19**, 163 (1984).

[28]S. L. Gilbert, R. N. Watts, and C. E. Wieman, Phys. Rev. A **27**, 581 (1983).

[29]R. Gupta, W. Happer, L. K. Lam, and S. Svanberg, Phys. Rev. A **8**, 2792 (1973).

[30]P. Goy, J. M. Raimond, G. Vitrant, and S. Haroche, Phys. Rev. A **26**, 2733 (1982).

[31]R. Gupta, Ninth International Conference on the Physics of Electron and Atomic Collisions, Seattle, 1975, edited by J. S. Risley and R. Geballe (Univeristy of Washington Press, Seattle, 1975), p. 712.

[32]J. Abele, Z. Phys. A **274**, 185 (1975).

[33]D. Feiertag, A. Sahm, and G. zu Putlitz, Z. Phys. **255**, 93

(1972).

[34]C. Tai, R. Gupta, and W. Happer, Phys. Rev. A **8**, 1661 (1973).

[35]P. Tsekeris, J. Farley, and R. Gupta, Phys. Rev. A **11**, 2202 (1975).

[36]J. Farley, P. Tsekeris, and R. Gupta, Phys. Rev. A **15**, 1530 (1977).

[37]The fitted formula for the $^2S_{1/2}[F=3-4]$ hyperfine (hf) interval applicable for all n is

$$\Delta_{hf}(^2S_{1/2})=52\,530/(n^*)^3+8204/(n^*)^5+63\,020/(n^*)^7 \ .$$

The corresponding formula for the $^2P_{1/2}[F=3-4]$ hyperfine interval is

$$\Delta_{hf}(^2P_{1/2})=14\,705/(n^*)^3-4895/(n^*)^5+28\,000/(n^*)^7 \ .$$

Here n^* is the effective quantum number calculated from the modified Ritz coefficients of Table V, and the hyperfine interval is given in megahertz.

[38]H. Heinke, J. Lawrenz, K. Niemax, and K.-H. Weber, Z. Phys. A **312**, 329 (1983).

[39]K. Bockasten, Phys. Rev. A **9**, 1087 (1974).

[40]K. Bockasten, J. Opt. Soc. Am. **54**, 1065 (1964).

[41]The hydrogenic fine-structure splitting is given by

$$\Delta(nl\,^2L)=[R\alpha^2/n^3l(l+1)] \ .$$

[42]K. Niemax (private communication).

[43]G. A. Ruff, K. A. Safinya, and T. F. Gallagher, Phys. Rev. A **22**, 183 (1980).

[44]T. J. McIlrath, J. Sugar, V. Kaufman, D. Cooper, and W. T. Hill III, J. Opt. Soc. Am. B **3**, 398 (1986).